

1 **Effects of ultraviolet radiation on photosynthetic performance and N<sub>2</sub> fixation in**  
2 ***Trichodesmium erythraeum* IMS 101**

3 **Xiaoni Cai<sup>1,2</sup>, David A. Hutchins<sup>2</sup>, Feixue Fu<sup>2</sup> and Kunshan Gao<sup>1\*</sup>**

4 <sup>1</sup>State Key Laboratory of Marine Environmental Science, Xiamen University, Xiamen,  
5 Fujian, 361102, China

6 <sup>2</sup>Department of Biological Sciences, University of Southern California, 3616 Trousdale  
7 Parkway, Los Angeles, California, 90089, USA

8

9 **Abstract**

10 Biological effects of ultraviolet radiation (UVR; 280–400 nm) on marine primary  
11 producers are of general concern, as oceanic carbon fixers that contribute to the marine  
12 biological CO<sub>2</sub> pump are being exposed to increasing UV irradiance due to global  
13 change and ozone depletion. We investigated the effects of UV-B (280-320 nm) and  
14 UV-A (320-400 nm) on the biogeochemically-critical filamentous marine N<sub>2</sub>-fixing  
15 cyanobacterium *Trichodesmium* (strain IMS101) using a solar simulator as well as  
16 under natural solar radiation. Short exposure to UV-B, UV-A, or integrated total UVR  
17 significantly reduced the effective quantum yield of photosystem II (PSII) and  
18 photosynthetic carbon and N<sub>2</sub> fixation rates. Cells acclimated to low light were more  
19 sensitive to UV exposure compared to high-light grown ones, which had more UV  
20 absorbing compounds, most likely mycosporine-like amino acids (MAAs). After  
21 acclimation under natural sunlight, the specific growth rate was lower (by up to 44%),  
22 MAAs content was higher, and average trichome length was shorter (by up to 22%) in  
23 the full spectrum of solar radiation with UVR, than under a photosynthetically active  
24 radiation (PAR) alone treatment (400-700 nm). These results suggest that prior  
25 shipboard experiments in UV-opaque containers may have substantially overestimated  
26 in-situ nitrogen fixation rates by *Trichodesmium*, and that natural and anthropogenic

27 elevation of UV radiation intensity could significantly inhibit this vital source of new  
28 nitrogen to the current and future oligotrophic oceans.

## 29 **Introduction**

30 Global warming is inducing shoaling of the upper mixed layer and enhancing a  
31 more frequent stratification of the surface layer, thus exposing phytoplankton cells  
32 which live in the upper mixed layer to higher depth-integrated irradiance including UV  
33 radiation (Häder and Gao, 2015). The increased levels of UV radiation have generated  
34 concern about their negative effects on aquatic living organisms, particularly  
35 phytoplankton, which require light for energy and biomass production.

36 Cyanobacteria are the largest and most widely distributed group of photosynthetic  
37 prokaryotes on the Earth, and they contribute markedly to global CO<sub>2</sub> and N<sub>2</sub> fixation  
38 (Sohm et al., 2011). Fossil evidence suggests that cyanobacteria first appeared during  
39 the Precambrian era (2.8 to 3.5 ×10<sup>9</sup> years ago) when the atmospheric ozone shield was  
40 absent (Sinha and Häder, 2008). Cyanobacteria have thus often been presumed to have  
41 evolved under more elevated UV radiation conditions than any other photosynthetic  
42 organisms, possibly making them better equipped to handle UV radiation.

43 Nevertheless, a number of studies have shown that UV-B not only impairs the  
44 DNA, pigmentation and protein structures of cyanobacteria, but also several key  
45 metabolic activities, including growth, survival, buoyancy, nitrogen metabolism, CO<sub>2</sub>  
46 uptake, and ribulose 1,5-bisphosphate carboxylase activity (Rastogi et al., 2014). To  
47 deal with UV stress cyanobacteria have evolved a number of defense strategies,  
48 including migration to escape from UV radiation, efficient DNA repair mechanisms,  
49 programmed cell death, the production of antioxidants, and the biosynthesis of UV-  
50 absorbing compounds, such as MAAs and scytonemin (Rastogi et al., 2014; Häder et  
51 al., 2015).

52 The non-heterocystous cyanobacterium *Trichodesmium* plays a critical role in the  
53 marine nitrogen cycle, as it is one of the major contributors to oceanic nitrogen fixation

54 (Capone et al., 1997) and furthermore is an important primary producer in the tropical  
55 and sub-tropical oligotrophic oceans (Carpenter et al., 2004). This global importance of  
56 *Trichodesmium* has motivated numerous studies regarding the physiological responses  
57 of *Trichodesmium* to environmental factors, including visible light, phosphorus, iron,  
58 temperature, and CO<sub>2</sub> (Kranz et al., 2010; Shi et al., 2012; Fu et al., 2014; Spungin et  
59 al., 2014; Hutchins et al., 2015). However, to the best of our knowledge, nothing has  
60 been documented about how UV exposure may affect *Trichodesmium*.

61 *Trichodesmium* spp. have a cosmopolitan distribution throughout much of the  
62 oligotrophic tropical and subtropical oceans, where there is a high penetration of solar  
63 UV-A and UV-B radiation (Carpenter et al., 2004). It also frequently forms extensive  
64 surface blooms (Westberry and Siegel, 2006), where it is presumably exposed to very  
65 high levels of UV radiation. Moreover, in the ocean, *Trichodesmium* populations may  
66 experience continuously changing irradiance intensities as a result of vertical mixing.  
67 Cells photoacclimated to reduced irradiance at lower depths might be subject to solar  
68 UVR damage when they are vertically delivered close to the sea surface due to mixing.  
69 Therefore, this unique cyanobacterium may have developed defensive mechanisms to  
70 overcome harmful effects of frequent exposures to intense UV radiation. Understanding  
71 how its N<sub>2</sub> fixation and photosynthesis respond to UV irradiance will thus further our  
72 knowledge of its ecological and biogeochemical roles in the ocean.

73 When estimating N<sub>2</sub> fixation using incubation experiments in the field, marine  
74 scientists have typically excluded UV radiation by using incubation bottles made of  
75 UV-opaque materials like polycarbonate (Capone et al., 1998; Olson et al., 2015). Thus,  
76 it seems possible that most shipboard measurements of *Trichodesmium* N<sub>2</sub> fixation rates  
77 could be overestimates of actual rates under natural UV exposure conditions in the  
78 surface ocean. Because of the importance of *Trichodesmium* in the input of carbon and  
79 nitrogen on oligotrophic oceans, and the lack of studies about the impact of enhanced  
80 UVR on the C and N fixation, is that we design the experiments. In this study,  
81 *Trichodesmium* was exposed to spectrally realistic irradiances of UVR in laboratory

82 experiments to examine the short-term effects of UVR on photosynthesis and N<sub>2</sub>  
83 fixation. In addition, *Trichodesmium* was grown under natural solar irradiance outdoors  
84 in order to assess UV impacts on longer timescales, and to test for induction of  
85 protective mechanisms to ameliorate chronic UV exposure effects.

86

## 87 **Materials and methods**

88 **Experimental design** The experiments to evaluate how UVR affects photosynthesis  
89 and N<sub>2</sub> fixation of *Trichodesmium* were carried on indoor and outdoor as follows: this  
90 study included two parts: (1) A short-term experiment under a solar stimulator (refer to  
91 Fig.S1 for the spectrum) to examine the responses of *Trichodesmium erythraeum* IMS  
92 101 to a range of acute UV radiation exposures, and (2) A long-term UV experiment  
93 under natural sunlight to examine acclimated growth and physiology of *Trichodesmium*  
94 IMS 101. The first set of experiments was intended to mimic intense but transitory UV  
95 exposures, as might occur sporadically during vertical mixing, while the second set was  
96 intended to give insights into responses during extended near-surface UV exposures,  
97 such as during a surface bloom event.

98 **Short-term UV experiment** *Trichodesmium erythraeum* IMS101 strain was isolated  
99 from the North Atlantic Ocean (Prufert-Bebout et al., 1993) and maintained in  
100 laboratory stock cultures in exponential growth phase in autoclaved artificial seawater  
101 enrich with nitrogen free YBCII medium (Chen et al., 1996). For the short-term UV  
102 experiment, the cells were grown under low light (LL) 70  $\mu\text{mol photons m}^{-2} \text{ s}^{-1}$  and  
103 high light (HL) 400  $\mu\text{mol photons m}^{-2} \text{ s}^{-1}$  (12:12 light: dark) of PAR for at least 50  
104 generations (about 180 days) prior to the UV experiments. These two light levels  
105 represent growth sub-saturating and super-saturating levels for *Trichodesmium* (Cai et  
106 al., 2015). Cultures were grown in triplicate using a dilute semi-continuous culture  
107 method, with medium renewed every 4-5 days at 25°C. The cell concentration was  
108 maintained at  $< 5 \times 10^4 \text{ cell ml}^{-1}$ .

109 To determine the short-term responses of *Trichodesmium* IMS101 to UV radiation,  
110 subcultures of *Trichodesmium* IMS101 were dispensed at a final cell density of  $2-4 \times$   
111  $10^4$  cells  $\text{ml}^{-1}$  into containers that allow transmission of all or part of the UV spectrum,  
112 including 35 ml quartz tubes (for measurements of carbon fixation or measurements of  
113 fluorescence parameters), 100 ml quartz tubes (for pigment measurements), or 13 ml  
114 gas-tight borosilicate glass vials (for  $\text{N}_2$  fixation measurements). Three triplicated  
115 radiation treatments were implemented: (1) PAB (PAR+UV-A+UV-B) treatment,  
116 using tubes covered with Ultraphan film 295 (Digefra, Munich, Germany), thus  
117 receiving irradiances  $>295$  nm; (2) PA (PAR+UV-A) treatment, using tubes covered  
118 with Folex 320 film (Montagefolie, Folex, Dreieich, Germany), and receiving  
119 irradiances  $>320$  nm; and (3) P treatment: tubes covered with Ultraphan film 395 (UV  
120 Opak, Digefra), with samples receiving irradiances above 395 nm, representing PAR  
121 (400-700 nm). Since the transmission spectrum of the borosilicate glass was similar to  
122 that of Ultraphan film 295, the borosilicate glass vials for  $\text{N}_2$  fixation measurements of  
123 PAB treatment were uncovered. Transmission spectra of these tubes (quartz and  
124 borosilicate) and the various cut-off foils used in this study are shown in Fig. S1.

125 The experimental tubes were placed under a solar simulator (Sol 1200W; Dr. Hönle,  
126 Martinsried, Germany) at a distance of 110 cm from the lamp, and maintained in a  
127 circulating water bath for temperature control ( $25^\circ\text{C}$ ) (CTP-3000, Eyela, Japan).  
128 Irradiance intensities were measured with a LI-COR  $2\pi$  PAR sensor (PMA2100, Solar  
129 light, USA) that has channels for PAR (400-700 nm), UV-A (320-400 nm) and UV-B  
130 (280-320 nm). Measured values at the 110 cm distance were  $87 \text{ Wm}^{-2}$  (PAR, ca. 400  
131  $\mu\text{mol photons m}^{-2} \text{ s}^{-1}$ ),  $28 \text{ Wm}^{-2}$  (UV-A) and  $1 \text{ Wm}^{-2}$  (UV-B), respectively. For the  
132 fluorescence measurements, samples were exposed under a solar simulator for 60 min  
133 and measurements of fluorescence parameters were performed during the exposure (see  
134 below). Due to analytical sensitivity issues, for the carbon and  $\text{N}_2$  incorporation  
135 measurements, the exposure duration was 2 hrs, and for the measurements of UVAC  
136 (UV-absorbing compounds) contents, the exposure time was 10 hrs.

137 **Long-term UV experiment** To assess the long-term effects of solar ultraviolet  
138 radiation on *Trichodesmium* IMS101, an outdoor experiment was carried during the  
139 winter (Jan 1<sup>st</sup> to Jan 26<sup>th</sup>, 2014) in subtropical Xiamen, China. 300-400 ml cell cultures  
140 were grown in 500 ml quartz vessels exposed to 100% daytime natural solar irradiance  
141 (surface ocean irradiance) (daytime PAR average of  $\sim 120\text{W m}^{-2}$ , highest PAR at noon  
142  $\sim 300\text{W m}^{-2}$ ). All of the quartz vessels were placed in a shallow water bath at 25°C using  
143 a temperature control system (CTP-3000, Eyela, Japan). Two triplicated radiation  
144 treatments were implemented: (1) treatment P: PAR alone (400-700 nm), tubes covered  
145 with Ultraphan film 395 (UV Opak, Digefra); (2) treatment PAB: PAR+UV-A+UV-B  
146 (295-700 nm), unwrapped quartz tubes. Incident solar radiation was continuously  
147 monitored with a broadband Eldonet filter radiometer (Eldonet XP, Real Time  
148 Computer, Mührendorf, Germany) that was placed near the water bath. Daily doses of  
149 solar PAR, UV-A and UV-B during the experiments are shown in Fig. S2. The  
150 photoperiod during the outdoor incubation was 11:13 light:dark (light period from 7:00-  
151 18:00 of local time). Cells were maintained in exponential growth phase (cell density  $<$   
152  $5 \times 10^4$ ), with dilutions (after sunset) every 4 days. All parameters were measured after  
153 acclimation under P or PAB radiation for a week.

154 In order to evaluate adaptation responses of *Trichodesmium* to natural solar  
155 irradiance, all parameters were obtained after one week acclimation outdoor. Specific  
156 growth rate ( $\mu$ ,  $\text{d}^{-1}$ ) of *Trichodesmium* IMS101 was determined based on the change in  
157 cell concentrations over 4 days during the 8-11<sup>th</sup> and 12-15<sup>th</sup> day using microscopic  
158 counts (Cai et al., 2015), the corresponding total dose from Day 8 to Day 11 and from  
159 Day 12 to Day 15 were 17.03 and 18.51  $\text{MJ m}^{-2}$ , respectively. Chl *a* content was  
160 measured at the 11<sup>th</sup>, 15<sup>th</sup> and 19<sup>th</sup> day, and Chl *a*-specific absorption spectrum was  
161 measured at the 18<sup>th</sup> day. Carbon and N<sub>2</sub> fixation rate were measured at 11:00-13:00 on  
162 the 18<sup>th</sup> day; the diel solar irradiance record on that day is given in Fig. S3. In order to  
163 separate the respective effects of UV-A and UV-B on carbon and N<sub>2</sub> fixation, a shift  
164 experiment was carried out: subcultures from either P or PAB treatments were

165 transferred into another P (PAR), PA (PAR+UV-A), PAB (PAR+UV-A+UV-B)  
166 treatment, which were marked as P', PA', PAB' treatments, respectively (namely P  
167 grown cells divided into P', PA', PAB' treatments; PAB grown cells also divided into P',  
168 PA', PAB' treatments). 35 ml quartz tubes and 13 ml gas-tight borosilicate glass vials  
169 were used for carbon and N<sub>2</sub> fixation measurements, respectively, as described below.  
170 Triplicate samples were used for each radiation treatment for carbon and N<sub>2</sub> fixation,  
171 and the incubations were performed under 100% solar irradiance for 2 hrs.

## 172 **Measurements and analyses**

173 **Effective photochemical quantum yield** Effective photochemical quantum yield  
174 ( $F_V'/F_M'$ ) is generally considered to be light quantum using efficiency. We use this  
175 parameter to indicate Photosystem II activity. During the exposure under the solar  
176 stimulator in the short-term experiment, small aliquots of cultures (2 ml) were  
177 withdrawn at time intervals of 3-10 min and immediately measured (without any dark  
178 adaptation) using a Pulse-Amplitude-Modulated (PAM) fluorometer (Xe-PAM, Walz,  
179 Germany). The quantum yield of PSII ( $F_V'/F_M'$ ) was determined by measuring the  
180 instant maximum fluorescence ( $F_M'$ ) and the steady state fluorescence ( $F_t$ ) under the  
181 actinic light. The maximum fluorescence ( $F_M'$ ) was determined using a saturating light  
182 pulse (4000  $\mu\text{mol photons m}^{-2} \text{s}^{-1}$  in 0.8 s) with the actinic light level set at 400  $\mu\text{mol}$   
183  $\text{photons m}^{-2} \text{s}^{-1}$ , similar to the PAR level during the solar simulator exposure The  
184 quantum yield was calculated as:  $F_V'/F_M' = (F_M' - F_t)/F_M'$  (Genty et al., 1989).

## 185 **Chlorophyll-specific absorption spectra and UV-absorbing compounds (UVACs)**

186 Chl *a*-specific absorption spectra were measured on the 18<sup>th</sup> day, after consecutive  
187 sunny days. Cellular absorption spectra were measured using the “quantitative filter  
188 technique” (Kiefer and SooHoo, 1982; Mitchell 1990). The cells were filtered onto GF/F  
189 glass fiber filters and scanned from 300 to 800 nm using a 1-nm slit in a  
190 spectrophotometer equipped with an integrating sphere to collect all the transmitted or  
191 forward-scattered light (i.e., light diffused by the filter and the quartz diffusing plate).

192 Filters soaked in culture medium were used as blanks. Chlorophyll-specific absorption  
193 cross-sections ( $a^*$ ) were calculated according to Cleveland and Weidemann (1993) and  
194 Anning et al., (2000). Content of Chl *a* and UV-absorbing compounds (UVACs) were  
195 measured by filtering the samples onto GF/F filters and subsequently extracted in 4 mL  
196 of 100% methanol overnight in darkness at 4 °C. The absorption of the supernatant was  
197 measured by a scanning spectrophotometer (Beckman Coulter Inc., Fullerton, CA,  
198 USA). The concentration of Chl *a* was calculated according to Ritchie (2006). The main  
199 absorption values for UV-absorbing compounds ranged between wavelengths of 310  
200 and 360 nm, and the peak absorption value at 332 nm was used to estimate total  
201 absorptivity of UVACs according to Dunlap et al., (1995). The absorptivity of UVACs  
202 was finally normalized to the Chl *a* content ( $\mu\text{g } (\mu\text{g Chl } a)^{-1}$ ).

203 *Trichodesmium* IMS101 UVACs content was compared to that of three other  
204 marine phytoplankton species, including *Chlorella*.sp, *Phaeodactylum tricorutum*,  
205 and *Synechococcus* WH7803, representing a green alga, a diatom and a unicellular  
206 cyanobacterium, respectively. All cultures were maintained under the same conditions  
207 (25°C, 150  $\mu\text{mol photons m}^{-2} \text{ s}^{-1}$ ) for several days prior to pigment extraction. The  
208 absorption spectra were measured as the same method in *Trichodesmium* by filtering  
209 the samples on GF/F filters that were subsequently extracted in 4 mL of 100% methanol  
210 overnight at 4 °C. The absorption spectra of the supernatant were scanned from 250 to  
211 800 nm in a spectrophotometer (Beckman Coulter Inc., Fullerton, CA, USA). The  
212 Optical Density (OD) values were then normalized to OD (662 nm), Chl *a* peak.

213 **Carbon fixation rates** Carbon fixation rate of both short- and long-term experiments  
214 were measured using the  $^{14}\text{C}$  method. A total of 20 ml samples were placed in 35 ml  
215 quartz tubes and inoculated with 5  $\mu\text{Ci}$  (0.185 MBq) of labeled sodium bicarbonate (ICN  
216 Radiochemicals), and were then maintained under the corresponding radiation  
217 treatments for 2 hrs. After incubation, the cells were filtered onto Whatman GF/F filters  
218 ( $\Phi$  25 mm) and stored at -20°C until analysis. To determine the radioactivity, the filters  
219 were thawed and then exposed to HCl fumes overnight and dried at 60°C for 4 hrs



220 before being placed in scintillation cocktail (Hisafe 3, Perkin-Elmer, Shelton, CT, USA),  
221 and measured with a scintillation counter (Tri-Carb 2800TR, Perkin-Elmer, Shelton,  
222 CT, USA) as previously described (Cai et al., 2015).

223 **N<sub>2</sub> fixation rates** Rates of N<sub>2</sub> fixation for both short- and long-term experiments were  
224 measured in parallel with the carbon fixation measurements using the acetylene  
225 reduction assay (ARA) (Capone et al., 1993). Samples of 5 ml subcultures were placed  
226 in 13 ml gas-tight borosilicate vials (described above), and 1ml acetylene was injected  
227 into the headspace before incubating for 2 hrs under the corresponding radiation  
228 treatment conditions. A 500 µl headspace sample was then analyzed in a gas  
229 chromatograph equipped with a flame-ionization detector and quantified relative to an  
230 ethylene standard. The ethylene produced was calculated using the Bunsen gas  
231 solubility coefficients according to Breitbarth et al., (2004) and an ethylene production  
232 to N<sub>2</sub> fixation conversion factor of 4 was used to derive N<sub>2</sub> fixation rates, which were  
233 then normalized to cell number.

234 **Data analysis** The inhibition of ΦPSII, carbon fixation and N<sub>2</sub> fixation due to UVR,  
235 UV-A, or UV-B was calculated as:

236 
$$\text{UVR-induced inhibition} = (I_P - I_{PAB})/I_P \times 100\%$$

237 
$$\text{UV-A-induced inhibition} = (I_P - I_{PA})/I_P \times 100\%$$

238 
$$\text{UV-B-induced inhibition} = \text{UVR}_{\text{inh}} - \text{UVA}_{\text{inh}}$$

239 where I<sub>P</sub>, I<sub>PA</sub>, I<sub>PAB</sub> indicate the values of carbon fixation or N<sub>2</sub> fixation in the P, PA  
240 and PAB treatments, respectively. Repair (r) and damage (k) rates during the 60 min  
241 exposure period in the presence of UV were calculated using the Kok model (Heraud  
242 and Beardall, 2000):

243 
$$P/P_{\text{initial}} = r/(r+k) + k/(r+k) \times \exp(-(r+k) \times t),$$

244 where P<sub>initial</sub> and P were the yield values at the beginning and at exposure time t.

245 Three replicates for culture conditions or each radiation condition was used in all

246 experiments, and the data are plotted as mean and standard deviation values. Two way  
247 ANOVA tests were used to determine the interaction between acclimatization  
248 conditions and UVR at a significance level of  $p=0.05$ .

249

## 250 **Results**

251 **Short-term UV experiment** The effects of acute UVR exposure on cells grown under  
252 LL and HL conditions are shown in Fig.1. For the cells grown under LL condition, the  
253  $F_V'/F_M'$  declined sharply within 10 min after first exposure in all radiation treatments,  
254 and then leveled off.  $F_V'/F_M'$  decreased less in the samples receiving PAR alone (to 43%  
255 of the initial value) than those additionally receiving UV-A (to 30% of the initial value)  
256 or UV-A+UV-B (to 24% of the initial value) (Fig.1A). The  $F_V'/F_M'$  value of PA and  
257 PAB treatments were significantly lower compared to the PAR treatment ( $p=0.03$  and  
258  $p<0.01$ , respectively).  $F_V'/F_M'$  of HL grown cells declined less and more slowly  
259 compared to the LL grown cells. The  $F_V'/F_M'$  of HL cells under PAR alone remained  
260 more or less constant during the exposure, since the PAR level was similar to the growth  
261 level of HL ( $400 \mu\text{mol photons m}^{-2} \text{ s}^{-1}$ ). In contrast, the  $F_V'/F_M'$  decreased to 75% and  
262 65% of its initial value for the PA and PAB treatment, respectively, and were  
263 significantly lower than the P treatment ( $p<0.01$ ) (Fig.1B).

264 The damage and repair rates of the PSII reaction center estimated from the  
265 exponential decay in the effective quantum yield showed higher damage and lower  
266 repair rates in the LL-grown cells than in the HL-grown ones (Fig.1C,D). The PSII  
267 damage rates ( $k$ ,  $\text{min}^{-1}$ ) of LL grown cells were 0.14, 0.16 and  $0.15 \text{ min}^{-1}$  in the P, PA  
268 and PAB treatments, respectively, about 2 times faster than in the cells grown under HL  
269 conditions (Fig.1C). The PSII repair rates ( $r$ ,  $\text{min}^{-1}$ ) of LL grown cells were 0.1, 0.06  
270 and  $0.05 \text{ min}^{-1}$  in the P, PA and PAB treatments, which were 83% ( $p<0.01$ ), 33% ( $p<0.01$ )  
271 and 54% ( $p<0.01$ ) lower than in HL grown cells, respectively (Fig.1D). The damage  
272 rate was not significantly different among P, PA and PAB treatments within either of

273 the LL- and HL-grown treatments ( $p>0.05$ ), but the repair rate was much higher in the  
274 P treatment without UV than in PA or PAB treatments in the HL-grown cells ( $p<0.01$ ).

275 The photosynthetic carbon fixation and  $N_2$  fixation rates during the UV exposure  
276 are shown in Fig. 2. The HL-grown cells had 17% higher photosynthetic carbon fixation  
277 rates than the LL-grown ones under the PA treatment ( $p<0.01$ ), however, the LL and  
278 HL-grown cells didn't show significant differences in carbon fixation rates under the P  
279 and PAB treatments ( $p=0.29$ , and  $p=0.06$ ). In the presence of UV radiation, carbon  
280 fixation was significantly inhibited in both LL and HL-grown cells (Fig.2A). Carbon  
281 fixation inhibition induced by UV-A was about 35-45%, much larger than that induced  
282 by UV-B, which caused only about a 10% inhibition of carbon fixation ( $p<0.01$ ). The  
283 UV-A exposed carbon fixation rate was significantly higher in the LL- grown cells than  
284 in HL grown cells ( $p<0.01$ ), while UV-B did not cause a significant difference in  
285 inhibition between the HL- and LL-grown cells ( $p=0.88$ ) (Fig. 2B).  $N_2$  fixation rates  
286 were about twofold higher in HL-grown cells in all radiation treatments (Fig.2C,  
287  $p<0.01$ ), but the UV-induced  $N_2$  fixation inhibition showed no significant differences  
288 between the LL and HL grown cells regardless of UV-A or UV-B exposures (Fig. 2D,  
289  $p=0.80$ ,  $0.62$ ,  $0.39$  for UVA-, UVB-, and UVR-induced inhibition, respectively).

290 Compared to other phytoplankton under the same growth conditions,  
291 *Trichodesmium* IMS101 had much higher absorbance in the UV region (300-400 nm)  
292 (Fig. 3A). In this study, the absorbance at 332 nm of HL-grown cells was about twofold  
293 higher compared to LL-grown ones (Fig. 3B). However, the cellular Chl *a* content (data  
294 not shown) and UVACs contents of both LL and HL grown cells did not present  
295 differences between radiation treatments after exposure to UV for 10 hrs (Fig. 3C).

296 **Long-term UV experiment** After being acclimated under full natural solar radiation  
297 for 7 days, the specific growth rates of cells grown under the PAB treatment were  
298  $0.15 \pm 0.01$  and  $0.14 \pm 0.06$  during the 8-11<sup>th</sup> day and 12-15<sup>th</sup> day periods, respectively.  
299 These growth rates were significantly lower by 44% and 39% compared to cells grown

300 under the P treatment, respectively (Fig.4A,  $p=0.014$  and  $p=0.03$ ). The mean trichome  
301 lengths of P treatment cells on the 11<sup>th</sup> and 15<sup>th</sup> day were  $758 \pm 56$  and  $726 \pm 19$   $\mu\text{m}$ , while  
302 addition of UVR significantly reduced the trichome length by 22% (Day 11<sup>th</sup>,  
303  $p=0.02$ ) and 11% (Day 15<sup>th</sup>,  $p=0.02$ ).

304 Analysis of the Chl *a* specific absorption spectra,  $a^*(\lambda)$ , demonstrated that UVR  
305 had a major effect on the absorbance of UV regions and phycobilisomes (Fig. 5). The  
306 optical absorption spectra revealed a series of peaks in the UV and visible wavelengths  
307 corresponding to the absorption peaks of UVACs at 332 nm, Chl *a* at 437 and 664 nm,  
308 phycourobilin (PUB) at 495 nm, phycoerythrobilin (PEB) at 545 nm,  
309 phycoerythrocyanin (PEC) at 569 nm, and phycocyanin (PC) at 627 nm. In the UV  
310 region, the  $a^*(\lambda)$  value was higher in the PAB treatment cultures than in the P treatment  
311 cultures (Fig. 5). The UVR treatments did not show clear effects on Chl *a* content  
312 compared to acclimation to P alone measured on different days (Fig. S3). However, the  
313 ratio of UVACs to Chl *a* was increased by 41% in the PAB compared to the P treatment  
314 ( $p<0.01$ ).

315 The cells grown in the long-term P and PAB treatments showed different responses  
316 for carbon and N<sub>2</sub> fixation after being transferred to short-term P', PA', and PAB'  
317 radiation treatments at noon on the 18<sup>th</sup> day (Fig. 6). P and PAB acclimated cells did  
318 not show significant differences in carbon fixation among all short-term P', PA', PAB'  
319 treatments (Fig. 6A,  $p=0.17$ ,  $p=0.22$ ,  $p=0.51$ , respectively), nor in the UV-induced  
320 inhibition of carbon fixation (Fig. 6B,  $p>0.05$ ). However, inhibition induced by UV-A  
321 at short exposures was about 58% in both P and PAB treatments and significantly higher  
322 than inhibition induced by UV-B radiation (Fig. 6B,  $p<0.01$ ).

323 N<sub>2</sub> fixation rates of P acclimated cells were significantly higher than PAB  
324 acclimated cells in all P', PA', and PAB' treatments (Fig. 6C,  $p<0.01$ ). The N<sub>2</sub> fixation  
325 inhibition induced by UV-A of PAB acclimated cells was 49%, significantly higher by  
326 47% than that of P acclimated cells ( $p=0.03$ ), while there was no significant difference

327 in UVB-induced N<sub>2</sub> fixation inhibition between P and PAB acclimated cells (Fig. 6D,  
328 p=0.62). The carbon fixation rates measured under P (P treated cells to P') and PAB  
329 (PAB treated cells to PAB') conditions were 89.2 and 47.1 fmol C cell<sup>-1</sup> h<sup>-1</sup>, respectively,  
330 while N<sub>2</sub> fixation rates measured under those conditions were 1.9 and 0.5 fmol N<sub>2</sub> cell<sup>-1</sup>  
331 h<sup>-1</sup>. UVR exposure lowered estimates of carbon and N<sub>2</sub> fixation rates by 47% and 65%,  
332 respectively.

333

### 334 **Discussion**

335 Our study shows that growth, photochemistry, photosynthesis and N<sub>2</sub> fixation in  
336 *Trichodesmium*.sp are all significantly inhibited by UVR, including both UV-A and UV-  
337 B. These effects occur in both short-term, acute exposures, as well as after extended  
338 exposures during acclimated growth. These results are ecologically relevant, since this  
339 cyanobacterium is routinely exposed to elevated solar irradiances in its tropical habitat  
340 either transiently, during vertical mixing, or over longer periods during surface blooms.  
341 *Trichodesmium* provides a biogeochemically-critical source of new N to open ocean  
342 food webs, so significant UV inhibition of its growth and N<sub>2</sub> fixation rates could have  
343 major consequences for ocean biology and carbon cycling.

344 Short exposure to UVR causes a significant decline in the quantum yield of  
345 photosystem II (PSII) fluorescence of *Trichodesmium*, that is consistent with damage  
346 to critical PSII proteins such as D1 in a brackish water cyanobacterium *Arthrospira*  
347 (*Spirulina*) *platensis* (Wu et al., 2011). UV-induced degradation of D1 proteins results  
348 in inactivation of PSII, leading to reduction in photosynthetic activity (Campbell et al.,  
349 1998). In addition, studies of various microbial mats have shown that Rubisco activity  
350 and supply of ATP and NADPH are inhibited under UV exposure, which might also  
351 lead to the reduction in photosynthetic carbon fixation (Cockell and Rothschild, 1999;  
352 Sinha et al., 1996, 1997).

353 Exposure to UVR had an impact on nitrogenase activity in *Trichodesmium*, since  
354 both the short- and the long-term UV exposure led to significant reduction of N<sub>2</sub> fixation  
355 of up to 30% (short-term) or ~60% (long-term) (Fig. 2D and 6D). Studies on the  
356 freshwater cyanobacterium *Anabaena*. sp (subg. *Dolichospermum*). showed a 57%  
357 decline in N<sub>2</sub> fixation rate after 30 min exposure to UVR of 3.65W (Lesser, 2007).  
358 Some rice-field cyanobacteria completely lost N<sub>2</sub> fixation activity after 25-40 min  
359 exposure to UV-B of 2.5 W (Kumar et al., 2003). In our results, long-term exposure to  
360 UV led to higher inhibition of N<sub>2</sub> fixation, implying that accumulated damage to the  
361 key N<sub>2</sub>-fixing enzyme, nitrogenase, could have occurred during the growth period under  
362 solar radiation in the presence of UVR.

363 Compared to N<sub>2</sub> fixation, UVR induced an even higher degree of inhibition of  
364 carbon fixation. The carbon fixation rate decreased by 50% in the presence of UVR.  
365 UV-A induced higher inhibition than UV-B, indicating that although UV-B photons  
366 (295-320 nm) are in general more energetic and damaging than UV-A (320-400 nm),  
367 the greater fluxes of UV-A caused more inhibition of carbon fixation, which was  
368 consistent with other studies of spectral dependence of UV effects (Cullen and Neale  
369 1994; Neale 2000). This finding is ecologically significant, since UV-A penetrates  
370 much deeper into clear open ocean and coastal seawater than does UV-B.

371 Compared to low light-grown cells, the high light-grown ones were more resistant  
372 to UVR, which was reflected in the lower PSII damage rate and faster recovery rate in  
373 the presence of UVR, as well as the significantly lower levels of carbon fixation  
374 inhibition caused by UV-A and/or UV-B. Such a reduced sensitivity to UVR coincided  
375 well with a significant increase in UV-absorbing compounds in the HL-grown cells  
376 compared to the LL-grown ones. Similar dependence of photosynthetic sensitivity to  
377 UV inhibition on growth light levels has been reported in other species of  
378 phytoplankton (Litchman and Neale, 2005; Sobrino and Neale, 2007). A red-tide  
379 dinoflagellate *Gymnodinium sanguineum* Hirasaka accumulates 14-fold MAAs in

380 high-light grown cells ( $76 \text{ W m}^{-2}$ ) than in low-light grown ones ( $15 \text{ W m}^{-2}$ ) and the  
381 former ones have lower sensitivity to UVR at wavelengths strongly absorbed by the  
382 MAAs (Neale et al., 1998). The sensitivity of PSII quantum yield to UV exposure in  
383 *Synechococcus* WH7803 was also less in high-light-grown versus low-light-grown  
384 cells (Garczarek et al., 2008). In addition, it has been observed that phytoplankton from  
385 turbid waters or acclimated to low-light conditions are more sensitive to UVR than  
386 those from clear waters (Villafane et al., 2004; Litchman and Neale, 2005; Helbing et  
387 al., 2015). These observations suggest that *Trichodesmium* sp. may acclimate to growth  
388 in the upper mixed layer by producing UV-absorbing compounds, making them more  
389 tolerant of UVR than cells living at deeper depths.

390 Although UVR can clearly cause damage to PSII and inhibit physiological  
391 processes in *Trichodesmium* sp., this cyanobacterium has evolved protective  
392 biochemical mechanisms to deal with UVR in their natural high-UV habitat. One  
393 important class of UV-absorbing substances are mycosporine-like amino acids (MAAs)  
394 and scytonemin. These compounds strongly absorb in the UV-A and/or UV-B region of  
395 the spectrum, and dissipate its energy as heat without forming reactive oxygen species,  
396 protecting the cells from UV and from photooxidative stress (Banaszak 2003). The  
397 “mycosporine-like amino acids” (MAAs), which have strong UV-absorption maxima  
398 between 310 and 362 nm (Sinha and Häder, 2008) as identified by HPLC in other  
399 studies, consist of a group of small, water-soluble compounds, including asterina-332  
400 ( $\lambda_{\text{max}}=332$ ) and shinorine ( $\lambda_{\text{max}}=334$ ), which are the most abundant, as well as  
401 mycosporine-glycine ( $\lambda_{\text{max}}=310$ ), porphyra-334 ( $\lambda_{\text{max}}=334$ ), and palythene  
402 ( $\lambda_{\text{max}}=360$ ) (Shick and Dunlap 2002; Subramaniam et al., 1999). As was found  
403 previously in *Trichodesmium* spp., high absorbance in the UV region is mainly due to  
404 the presence of “mycosporinelike amino acids” (MAAs), with absorbance maxima  
405 between 310~362 nm (Sinha and Häder, 2008).

406 Our investigation strongly suggests that *Trichodesmium* is able to synthesize  
407 MAAs ( $\lambda_{\text{max}} \sim 330 \text{ nm}$  and  $360 \text{ nm}$ ) in response to elevated PAR and UVR. Synthesis

408 of MAAs has been reported to be stimulated by high PAR and UVR in other  
409 phytoplankton (Karsten et al., 1998; Vernet and Whitehead, 1996; Sinha et al., 2001).  
410 Our high light-grown cells were more tolerant of UVR, likely at least partly due to their  
411 ability to synthesize double the amount of MAAs in comparison to low light-grown  
412 ones (Fig.3B). It has been showed that accumulation of MAAs may represent a natural  
413 defensive system against exposure to biologically harmful UVR (Karsten et al., 1998)  
414 and cells with high concentrations of MAAs are more resistant to UVR than cells with  
415 small amounts of these compounds (Garcia-Pichel and Castenholz, 1993). In fact,  
416 MAAs concentrations varying between 0.9 and 8.4 ug mg (dry weight)<sup>-1</sup> have been  
417 measured in cyanobacterial isolates (Garcia-Pichel and Castenholz, 1993), and ratios of  
418 MAAs to Chl *a* in the range from 0.04 to 0.19 have been reported in cyanobacterial  
419 mats (Quesada et al., 1999). In our study, we found that *Trichodesmium* contained a  
420 much higher concentration of MAAs (the highest value in HL-grown cells is 5 pg cell<sup>-1</sup>)  
421 and that the ratio of these compounds to Chl *a* was 5, was consisted with previous  
422 reports in regard to *Trichodesmium* (Subramaniam et al., 1999), which is much higher  
423 than in other phytoplankton. This acclimatization capacity depending on intensity and  
424 spectral quality of radiation could be a major reason for the ability of *Trichodesmium*  
425 to grow and form extensive surface blooms under strong irradiation in the oligotrophic  
426 oceans.

427 In our study, no significant changes in the amount of MAAs were observed after  
428 10 h of exposure to UVR under the solar simulator. In contrast, a significant increase  
429 of 23% in the concentration of MAAs was observed in full solar spectrum treated cells  
430 compared to PAR-treated ones grown outdoors after consecutive sunny days (on the  
431 18<sup>th</sup>). It seems that the synthesis of MAAs takes a relatively long time. Other studies  
432 have shown the time required for induction of MAAs in other cyanobacteria is  
433 dependent on UV doses and species, and shows a circadian rhythm (Sinha et al., 2001;  
434 Sinha et al., 2003).

435 Not only did long-term exposure to high solar UVR significantly reduce



436 *Trichodesmium*'s growth rate (by 37~44%), but it also significantly shortened its  
437 average trichome length (less cell per filament) (Fig. 4). The decreased growth rates  
438 correlated with decreased trichome length are consistent with our previous studies  
439 under different light levels without UVR (Cai et al., 2015). It has been reported that  
440 enhanced UVR is one of the environmental factors that not only inhibit the growth of  
441 cyanobacteria, but also change their morphology (Rastogi et al., 2014). Natural solar  
442 UVR can suppress formation of heterocysts and shorten the filament length of  
443 *Anabaena* sp. PCC7120, because UVR may affect calcium signaling then the  
444 expression of the key genes responsible for cell differentiation (Gao et al., 2007).  
445 Natural levels of solar UVR in the Southern China were also found to break the  
446 filaments and alter the spiral structure of *Arthrospira (Spirulina) platensis*, with a  
447 compressed helix that lessens UV exposures for the cells (Wu et al., 2005). Cells in the  
448 trichomes of the estuarine cyanobacterium *Lyngbya aestuarii* coil and then form small  
449 bundles in response to UV-B irradiation (Rath and Adhikari, 2007). However, the  
450 shortened trichomes of *Trichodesmium* in this work may be a result of UV-inhibited  
451 growth rather than a responsive strategy against UV.

452 Carbon fixation in the long-term experiment showed similar patterns with the  
453 short-term UV experiment, demonstrating that UV-A played a larger role in inhibiting  
454 carbon fixation than UV-B. Since the ratio of UV-B to UV-A is lower in natural solar  
455 light (1:50) than under our artificial UVR (1:28), the inhibitory effects of UV-B were  
456 smaller compared to UV-A in the cultures under sunlight. Carbon fixation and N<sub>2</sub>  
457 fixation rates measured outdoors indicated that UV-induced carbon fixation inhibition  
458 recovers quickly following transfer to PAR conditions, while the UV-induced N<sub>2</sub>  
459 fixation inhibition does not (Fig.6AC). Factors that might be responsible include lower  
460 turnover rate of nitrogenase than that of RuBisco; more UV-induced damage to  
461 nitrogenase with lower efficiency of repair (Kumar et al., 2003); and indirect harm  
462 caused by ROS (Reactive Oxygen Species) induced by UV (Singh et al., 2014).

463 The UV effects in our study were measured under conditions that minimized self-

464 shading, namely during growth as single filaments. However, in its natural habitat  
465 *Trichodesmium* often grows in a colonial form, with packages of many cells held  
466 together by an extracellular sheath (Capone et al., 1998). In such colonial growth forms,  
467 the effective cellular pathlengths for UVR are likely greatly increased, thereby  
468 amplifying the overall sunscreen factor for the colony. *Trichodesmium.spp* might use  
469 this colony strategy to protect themselves from natural UV damage in the ocean.

470 Our investigation shows that this cyanobacterium appears to have evolved the  
471 ability to produce exceptionally high levels of UV protective compounds, likely  
472 mycosporine-like amino acids. However, even this protective mechanism is insufficient  
473 to prevent substantial inhibition of nitrogen and carbon fixation in the high-irradiance  
474 environment where this genus lives. *Trichodesmium* spp are distributed in the upper  
475 layers of the euphotic zone in oligotrophic waters, and its population densities are  
476 generally greatest at relatively shallow depths (20 to 40 m) in the upper water column  
477 (Capone et al., 1997). It seems likely that UV inhibition therefore significantly reduces  
478 the amount of critical new nitrogen supplied by *Trichodesmium* to the N-limited  
479 oligotrophic gyre ecosystems, a possibility that has not been generally considered in  
480 regional or global models of the marine nitrogen cycle. On the other hand, the UV  
481 absorbing compounds (most likely MAAs) are expensive to make in terms of nitrogen  
482 in particular (Singh et al., 2008). Decreased nitrogen supplied may increase sensitivity  
483 of phytoplankton assemblages to UV further (Litchman et al 2002), thus potentially  
484 creating a positive feedback between N-limitation and the UV sensitivity.

485 *Trichodesmium* can form dense, extensive blooms in the surface oceans, and a  
486 frequently cited estimate of global nitrogen fixation rates by *Trichodesmium* blooms is  
487  $\sim 42 \text{ Tg N yr}^{-1}$  (Westberry et al., 2006). Previous biogeochemical models of global  $\text{N}_2$   
488 fixation have emphasized controls by many environmental factors, including solar PAR,  
489 temperature, wind speed, and nutrient concentrations (Luo et al., 2014), but have largely  
490 neglected the effects of UVR. When estimating  $\text{N}_2$  fixation using incubation  
491 experiments in the field, however, marine scientists have typically excluded UVR by

492 using incubation bottles made of UV-opaque materials like polycarbonate (Olson et al.,  
493 2015). Our results suggest that under solar radiation at the surface ocean, including  
494 realistic levels of UVR inhibition lowers estimates of carbon fixation and N<sub>2</sub> fixation  
495 by around 47% and 65%, respectively (Fig.6).

496 Thus, it seems likely that shipboard measurements and possibly current model  
497 projections of *Trichodesmium* N<sub>2</sub> fixation and primary production rates that do not take  
498 into account UV inhibition could be substantial overestimates. However, our study was  
499 only carried out under full solar radiation, simulating sea surface conditions, so further  
500 studies are needed to investigate depth-integrated UV inhibition. Moreover, the  
501 response to UVR may be taxon-specific. For example, unicellular N<sub>2</sub>-fixing  
502 cyanobacteria such as the genus *Crocospaera*, with smaller cell size and thus greater  
503 light permeability, may be more vulnerable to UVR than *Trichodesmium* (Wu et al.,  
504 2015). In the future, as enhanced stratification and decreasing mixed layer depth expose  
505 cells to relatively higher UV levels, differential sensitivities to UVR may result in  
506 changes in diazotroph community composition. Such UV-mediated assemblage shifts  
507 could have potentially major consequences for marine productivity, and for the global  
508 biogeochemical cycles of nitrogen and carbon, future research that would be necessary  
509 to confirm and/or deepen the consequences of UV effects in carbon and nitrogen cycle  
510 in the ocean.

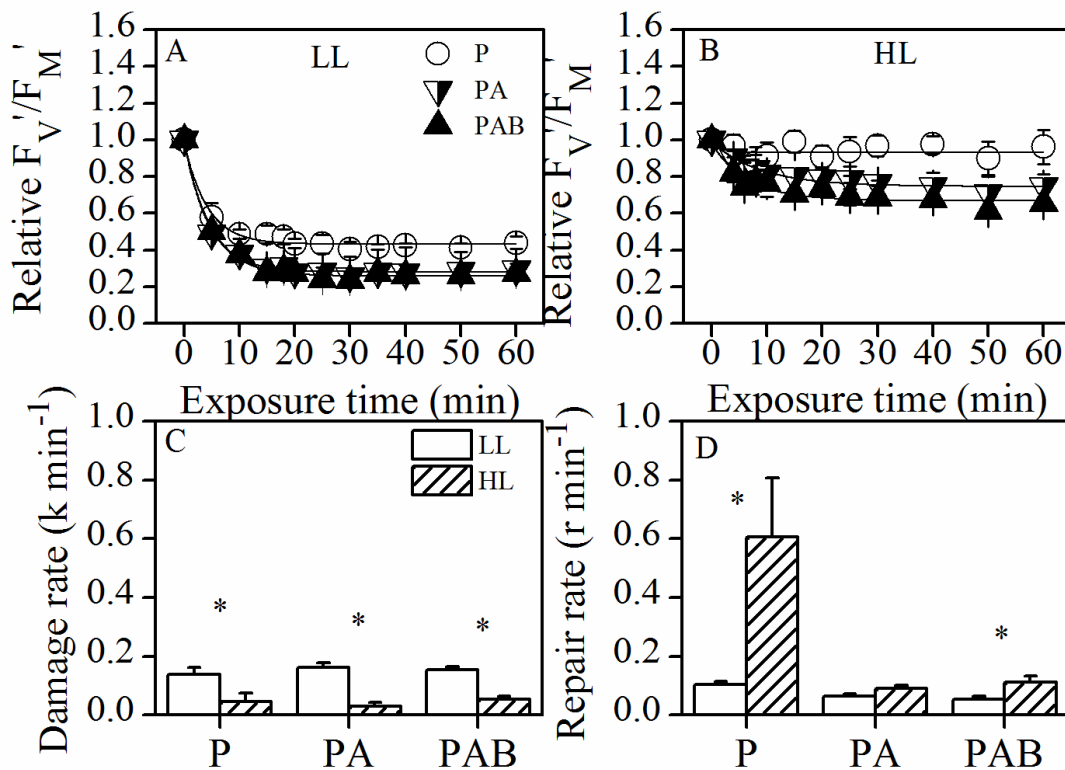
511

## 512 **Acknowledgements**

513 This study was supported by the National Key Research Programs 2016YFA0601400  
514 and National Natural Science Foundation (41430967; 41120164007) to KSG, and by  
515 U.S. National Science Foundation grants OCE 1260490 and OCE 1538525 to F-X.F.  
516 and D.A.H. DAH and F-X.F.'s visit to Xiamen was supported by MEL's visiting  
517 scientists programs. The authors would like to thank Nana Liu and Xiangqi Yi from  
518 Xiamen University for their kind assistance during the experiments.

519

520 **Figures**



521

522 Fig.1 Changes of effective quantum yield ( $F_V'/F_M'$ ) of *Trichodesmium* IMS101 grown  
523 under (A) LL and (B) HL conditions while exposed to PAR (P), PAR+UVA (PA) and  
524 PAR+UVA+UVB (PAB) under solar simulator for 60 min. PSII damage (C; k, in min<sup>-1</sup>)  
525 and repair rates (D; r, in min<sup>-1</sup>) of LL- and HL-grown cells were derived from the  
526 yield decline curve in the upper panels. Asterisks above the histogram bars indicate  
527 significant differences between LL- and HL-grown cells. Values are the mean  $\pm$ SD,  
528 triplicate incubations.

529

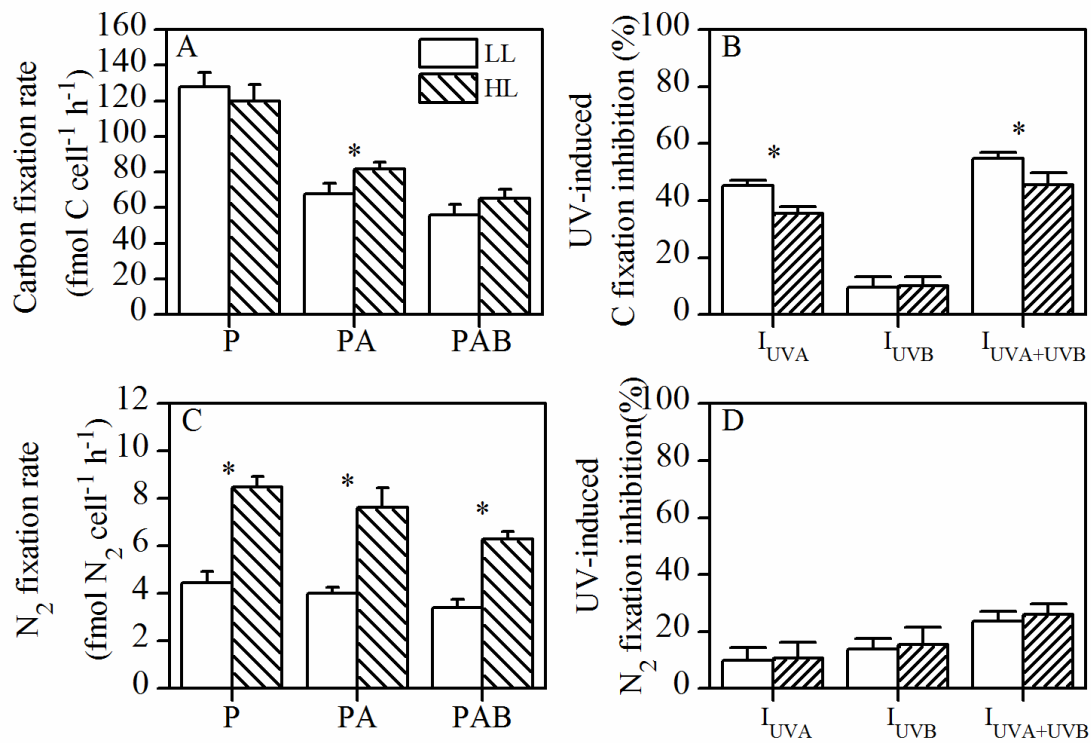
530

531

532

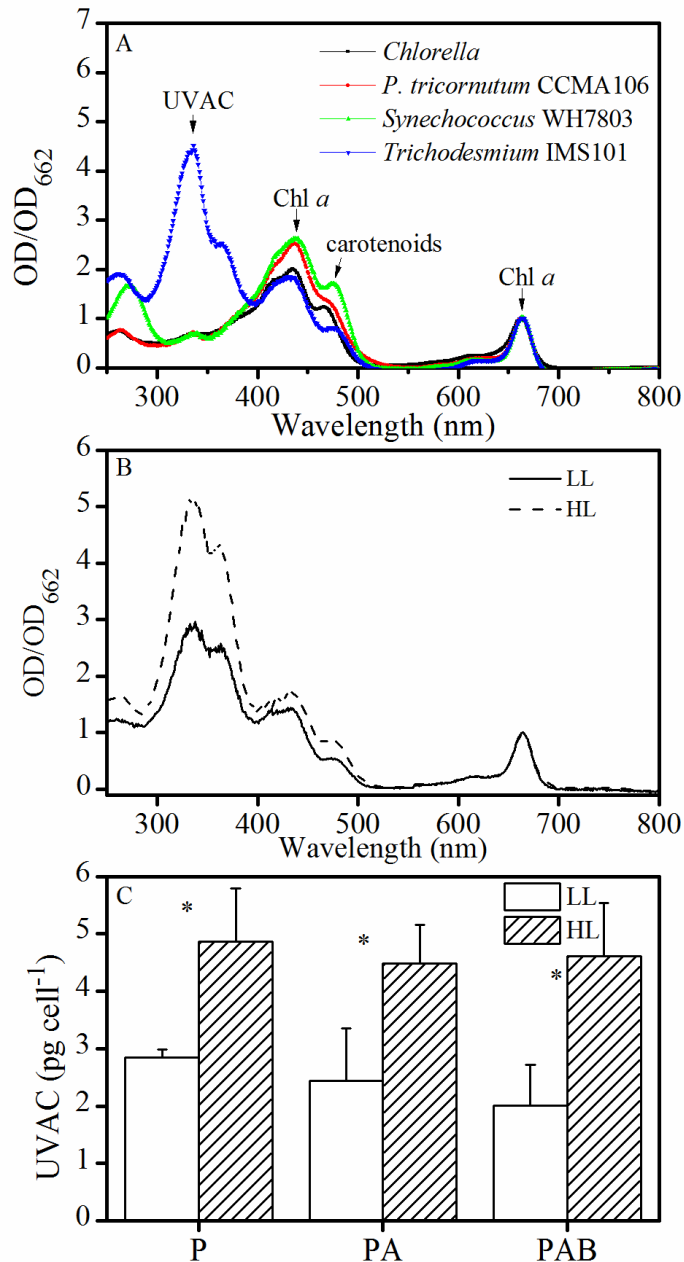
533

534



536

537 Fig.2 Photosynthetic carbon fixation rate (A; fmol C cell<sup>-1</sup> h<sup>-1</sup>) and UV-induced C  
 538 fixation inhibition (B), N<sub>2</sub> fixation rate (C; fmol N<sub>2</sub> cell<sup>-1</sup> h<sup>-1</sup>) and corresponding UV-  
 539 induced N<sub>2</sub> fixation inhibition (D) of *Trichodesmium* IMS101 grown under LL and HL  
 540 conditions. Asterisks above the histogram bars indicate significant differences between  
 541 LL- and HL-grown cells. Values are the mean  $\pm$ SD, triplicate incubations.



542

543 Fig.3 (A) Absorption spectrum of *Trichodesmium* IMS101 compared to other

544 phytoplankton. Pigments were extract by 100% methanol. OD value normalized to

545 OD<sub>662</sub> (Chl *a*). (B) Absorption spectrum of the *Trichodesmium* IMS101 grown under

546 LL and HL conditions, OD value normalized to OD<sub>662</sub> (Chl *a*).

547 UVACs of *Trichodesmium* IMS101 grown under LL and HL conditions after exposure

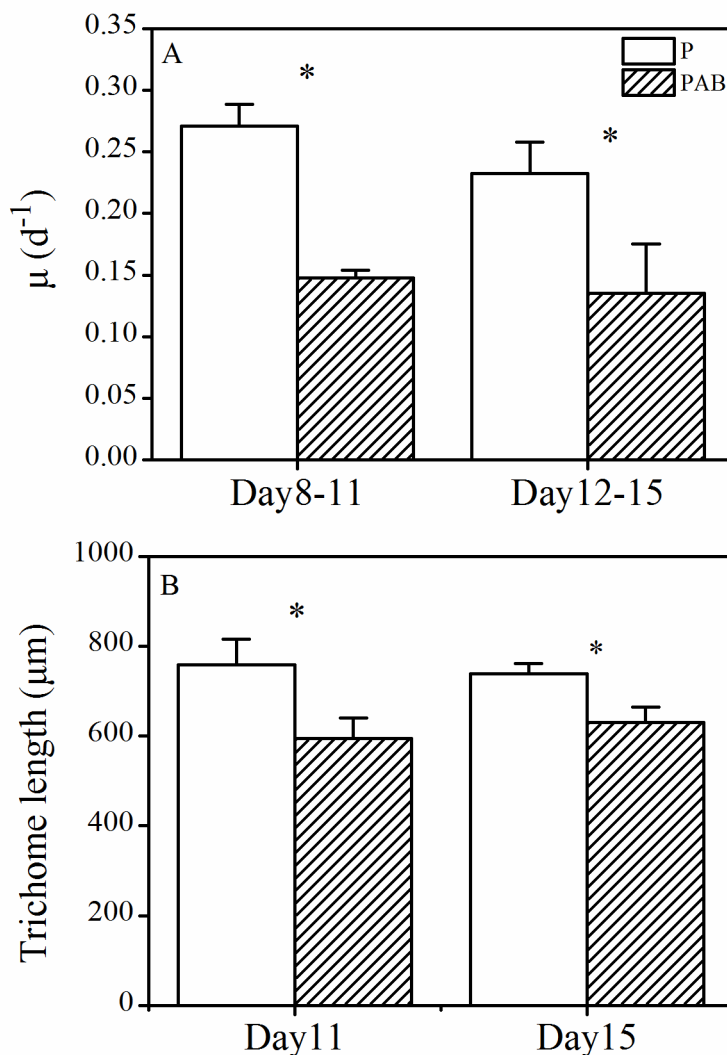
548 to PAR (P), PAR+UVA (PA), PAR+UVA+UVB (PAB) under solar stimulator for 10 h.

549 Asterisks above the histogram bars indicate significant differences between LL- and

550 HL-grown cells. Values are the mean  $\pm$ SD, triplicate incubations.

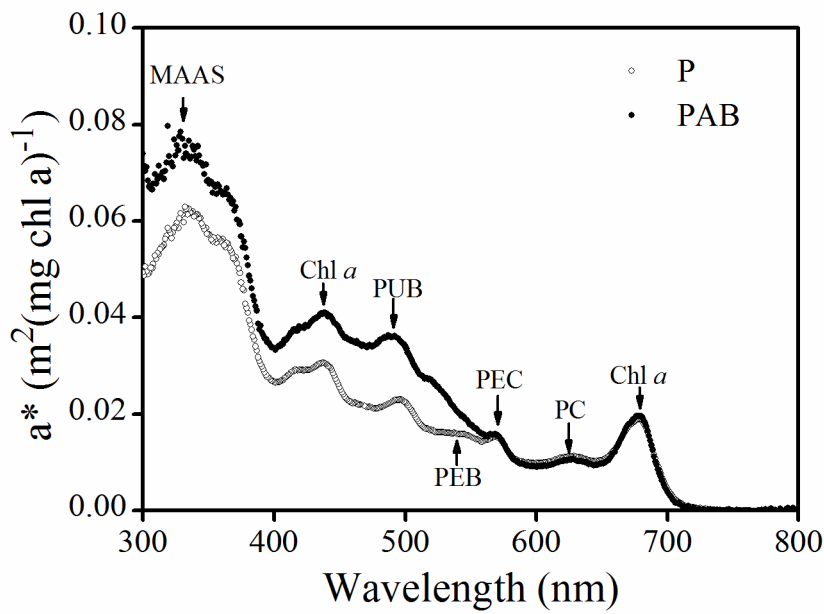
551

552



553

554 Fig.4 (A) Specific growth rate (measured during 8<sup>th</sup>-11<sup>th</sup> and 12<sup>th</sup>-15<sup>th</sup> day) of  
555 *Trichodesmium* IMS101 grown under solar PAR (P) and PAR+UVA+UVB (PAB).  
556 Corresponding total solar doses from Day 8 to Day 11 and from Day 12 to Day 15 were  
557 17.03 and 18.51 MJ, respectively. (B) Trichome length (measured on the 11<sup>th</sup> and 15<sup>th</sup>  
558 day) of *Trichodesmium* IMS101 grown under solar PAR (P) and PAR+UVA+UVB  
559 (PAB). The asterisks indicate significant differences between radiation treatments.  
560 Values are the mean  $\pm$ SD, triplicate cultures.



561

562 Fig.5 Chl *a* specific absorption spectrum ( $a^*$ ) of *Trichodesmium* IMS101 grown under  
 563 solar PAR (P) and PAR+UVA+UVB (PAB). The measurements were taken on the 18<sup>th</sup>  
 564 day. The absorption peaks of MAAs (330 nm), PUB (495 nm), PEB (545 nm), PEC  
 565 (569 nm), PC (625nm) and Chl *a* (438 and 664 nm) are indicated.

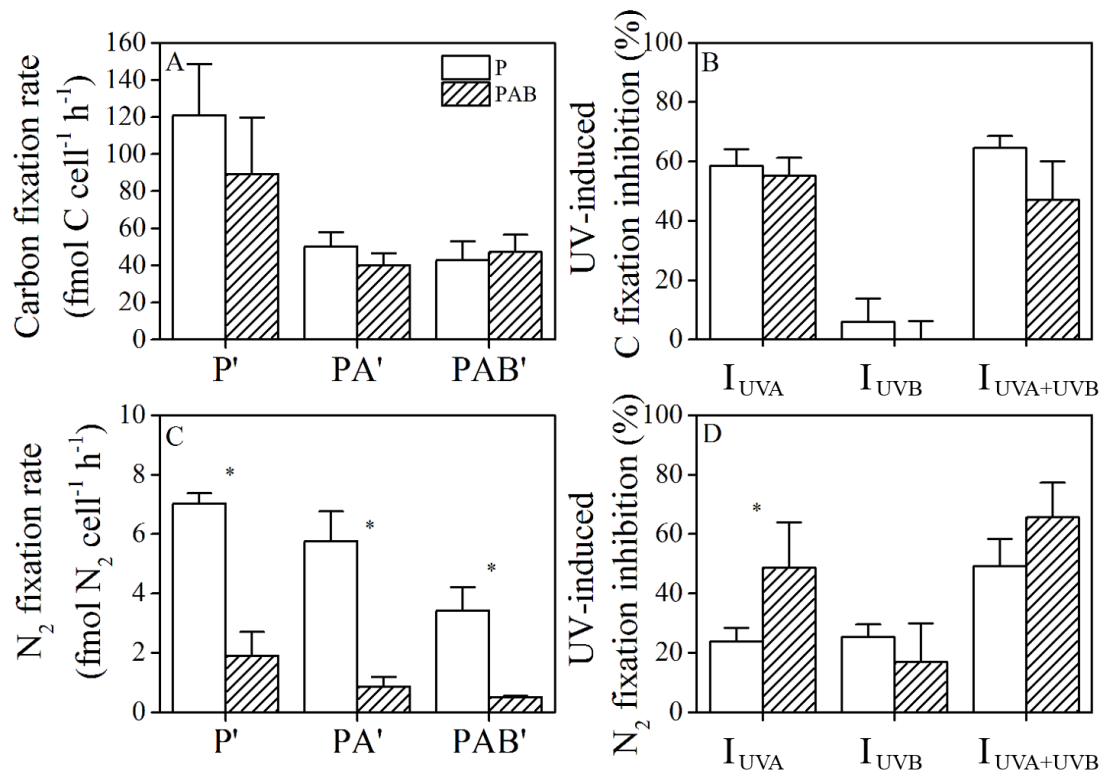
566

567

568

569





570

571 Fig. 6 Photosynthetic carbon fixation rate (A; fmol C cell<sup>-1</sup> h<sup>-1</sup>) and UV-induced C  
 572 fixation inhibition (B), N<sub>2</sub> fixation rate (C; fmol N<sub>2</sub> cell<sup>-1</sup> h<sup>-1</sup>) and corresponding UV-  
 573 induced N<sub>2</sub> fixation inhibition (D) of *Trichodesmium* IMS101 grown under solar PAR  
 574 (P) and PAR+UVA+UVB (PAB) transferred to another P', PA', PAB' treatments. The  
 575 measurement was taken on the 18<sup>th</sup> day at 11:00~13:00. Asterisks above the histogram  
 576 bars indicate significant differences between P and PAB treatments. Values are the mean  
 577 ±SD, triplicate incubations.

578

579

580

581

582

583

584

585

586

587

588 **References**

- 589 1. Anning, T., MacIntyre, H. L., Sammes, S. M. P. a. P. J., Gibb, S., and Geider, R. J.:  
590 Photoacclimation in the marine diatom *Skeletonema costatum*, *Limnol Oceanogr*,  
591 1807-1817, 2000.
- 592 2. Bouchard, J. N., Roy, S., and Campbell, D. A.: UVB Effects on the Photosystem  
593 II - D1 Protein of Phytoplankton and Natural Phytoplankton Communities,  
594 *Photochem Photobiol*, 82, 936-951, 2006.
- 595 3. Breitbarth, E., Mills, M. M., Friedrichs, G., and LaRoche, J.: The Bunsen gas  
596 solubility coefficient of ethylene as a function of temperature and salinity and its  
597 importance for nitrogen fixation assays, *Limnol. Oceanogr. Methods*, 2, 282-288,  
598 2004.
- 599 4. Cai, X., Gao, K., Fu, F., Campbell, D., Beardall, J., and Hutchins, D.: Electron  
600 transport kinetics in the diazotrophic cyanobacterium *Trichodesmium* spp. grown  
601 across a range of light levels, *Photosyn. Res.*, 124, 45-56, 10.1007/s11120-015-  
602 0081-5, 2015.
- 603 5. Campbell, D., Eriksson, M. J., Oquist, G., Gustafsson, P., and Clarke, a. K.: The  
604 cyanobacterium *Synechococcus* resists UV-B by exchanging photosystem II  
605 reaction-center D1 proteins., *Proceedings of the National Academy of Sciences* 95,  
606 364-369, 1998.
- 607 6. Capone, D.: Determination of nitrogenase activity in aquatic samples using the  
608 acetylene reduction procedure, In P. F. Kemp, B. F. Sherr, E. B. Sherr, and J. J.  
609 Cole (ed.), *Handbook of methods in aquatic microbial ecology*. Lewis Publishers,  
610 Boca Raton, Fla, p. 621–631, 1993.
- 611 7. Capone, D., Zehr, J., Paerl, H., and Bergman, B.: *Trichodesmium*, a globally  
612 significant marine cyanobacterium, *Science*, 276, 1221-1227, 1997.
- 613 8. Capone, D. G., Subramaniaml, A., Joseph, P., Carpenters, E. J., Johansen, M., and

- 614 Ronald, L.: An extensive bloom of the N<sub>2</sub>-fixing cyanobacterium *Trichodesmium*  
615 *erythraeum* in the central Arabian Sea, *Mar. Ecol. Prog. Ser.*, 172, 281-292, 1998.
- 616 9. Carpenter, E. J., Subramaniam, A., and Capone, D. G.: Biomass and primary  
617 productivity of the cyanobacterium *Trichodesmium* spp. in the tropical N Atlantic  
618 ocean, *Deep Sea Research Part I: Oceanographic Research Papers*, 51, 173-203,  
619 10.1016/j.dsr.2003.10.006, 2004.
- 620 10. Chen, Y. B., Zehr, J. P., and Mellon, M.: Growth and nitrogen fixation of the  
621 diazotrophic filamentous nonheterocystous cyanobacterium *Trichodesmium* sp.  
622 IMS101 in defined media: evidence for a circadian rhythm, *J Phycol*, 32, 916-923,  
623 1996.
- 624 11. Cleveland, J. S., and Weidemann, A. D.: Quantifying Absorption by Aquatic  
625 Particles: A Multiple Scattering Correction for Glass-Fiber, *Limnol Oceanogr*, 38,  
626 1321-1327, 1993.
- 627 12. Cockell, C. S., and Rothschild, L. J.: The Effects of UV Radiation A and B on  
628 Diurnal Variation in Photosynthesis in Three Taxonomically and Ecologically  
629 Diverse Microbial Mats, *Photochem Photobiol*, 69, 203-210, 10.1111/j.1751-  
630 1097.1999.tb03274.x, 1999.
- 631 13. Cullen, J. J., and Neale, P. J.: Ultraviolet radiation, ozone depletion, and marine  
632 photosynthesis, *Photosyn. Res.*, 39, 303-320, 10.1007/bf00014589, 1994.
- 633 14. Dunlap, W., Rae, G., Helbling, E., Villafañe, V., and Holm-Hansen, O.: Ultraviolet-  
634 absorbing compounds in natural assemblages of Antarctic phytoplankton, *Antarct*  
635 *J U S*, 30, 323-326, 1995.
- 636 15. Fay, P.: Oxygen relations of nitrogen fixation in cyanobacteria, *Microbiol. Rev.*, 56,  
637 340-373, 1992.
- 638 16. Fu, F.-X., Yu, E., Garcia, N. S., Gale, J., Luo, Y., Webb, E. A., and Hutchins, D. A.:  
639 Differing responses of marine N<sub>2</sub> fixers to warming and consequences for future  
640 diazotroph community structure, *Aquat. Microb. Ecol.*, 72, 33-46, 2014.
- 641 17. Garcia-Pichel, F., and W.Castenholz, R.: Occurrence of UV-

- 642 absorbingmycosporine-like compounds among cyanobacterial isolates and  
643 estimationof their screening capacity, *Appl. Environ. Microbiol.*, 163-169, 1993.
- 644 18. Genty, B., Briantais, J.-M., and Baker, N. R.: The relationship between the quantum  
645 yield of photosynthetic electron transport and quenching of chlorophyll  
646 fluorescence, *Biochimica et Biophysica Acta (BBA) - General Subjects*, 990, 87-  
647 92, [http://dx.doi.org/10.1016/S0304-4165\(89\)80016-9](http://dx.doi.org/10.1016/S0304-4165(89)80016-9), 1989.
- 648 19. Häder, D.-P., and Gao, K.: Interactions of anthropogenic stress factors on marine  
649 phytoplankton, *Frontiers in Environmental Science*, 3, 1-14, 2015.
- 650 20. Häder, D. P., Williamson, C. E., Wangberg, S. A., Rautio, M., Rose, K. C., Gao, K.,  
651 Helbling, E. W., Sinha, R. P., and Worrest, R.: Effects of UV radiation on aquatic  
652 ecosystems and interactions with other environmental factors, *Photochem.*  
653 *Photobiol. Sci.*, 14, 108-126, [10.1039/c4pp90035a](https://doi.org/10.1039/c4pp90035a), 2015.
- 654 21. He, Y.-Y., Klisch, M., and Häder, D.-P.: Adaptation of cyanobacteria to UV-B stress  
655 correlated with oxidative stress and oxidative damage., *Photochem Photobiol*, 76,  
656 188-196, 2002.
- 657 22. Heraud, P., and Beardall, J.: Changes in chlorophyll fluorescence during exposure  
658 of *Dunaliella tertiolecta* to UV radiation indicate a dynamic interaction between  
659 damage and repair processes, *Photosyn. Res.*, 63, 123-134,  
660 [10.1023/a:1006319802047](https://doi.org/10.1023/a:1006319802047), 2000.
- 661 23. Hutchins, D. A., Walworth, N. G., Webb, E. A., Saito, M. A., Moran, D., McIlvin,  
662 M. R., Gale, J., and Fu, F.-X.: Irreversibly increased nitrogen fixation in  
663 *Trichodesmium* experimentally adapted to elevated carbon dioxide, *Nature*  
664 *Communication*, 6, 8155, [10.1038/ncomms9155](https://doi.org/10.1038/ncomms9155), 2015.
- 665 24. Karsten, U., Sawall, T., and Wiencke, C.: A survey of the distribution of UV-  
666 absorbing substances in tropical macroalgae, *Phycol. Res.*, 46, 271-279,  
667 [10.1046/j.1440-1835.1998.00144.x](https://doi.org/10.1046/j.1440-1835.1998.00144.x), 1998.
- 668 25. Kiefer, D. A., and SooHoo, J. B.: Spectral absorption by marine particles of coastal  
669 waters of Baja California, *Limnol Oceanogr*, 27, 492-499, 1982.

- 670 26. Kranz, S. A., Levitan, O., Richter, K. U., Prasil, O., Berman-Frank, I., and Rost, B.:  
671 Combined effects of CO<sub>2</sub> and light on the N<sub>2</sub>-fixing cyanobacterium  
672 *Trichodesmium* IMS101: physiological responses, *Plant Physiol.*, 154, 334-345,  
673 10.1104/pp.110.159145, 2010.
- 674 27. Kumar, A., Tyagi, M. B., Jha, P. N., Srinivas, G., and Singh, A.: Inactivation of  
675 cyanobacterial nitrogenase after exposure to Ultraviolet-B radiation, *Curr.*  
676 *Microbiol.*, 46, 380-384, 10.1007/s00284-001-3894-8, 2003.
- 677 28. Litchman, Elena, Patrick J. Neale, and Anastazia T. Banaszak.: Increased  
678 sensitivity to ultraviolet radiation in nitrogen-limited dinoflagellates:  
679 Photoprotection and repair, *Limnol Oceanogr*, 47, 86-94, 2002.
- 680 29. Lesser, M. P.: Effects of ultraviolet radiation on productivity and nitrogen fixation  
681 in the Cyanobacterium, *Anabaena* sp. (Newton's strain), *Hydrobiologia*, 598, 1-9,  
682 10.1007/s10750-007-9126-x, 2007.
- 683 30. Luo, Y.-W., Lima, I. D., Karl, D. M., and Doney, S. C.: Data-based assessment of  
684 environmental controls on global marine nitrogen fixation, *BGeo*, 11, 619-708,  
685 2014.
- 686 31. Mitchell, B. G.: Algorithms for determining the absorption coefficient for aquatic  
687 particulates using the quantitative filter technique, Orlando'90, 16-20 April, 1990,  
688 137-148,
- 689 32. Neale, Patrick J., Anastazia T. Banaszak, and Catherine R. Jarriel.: Ultraviolet  
690 sunscreens in *Gymnodinium sanguineum* (Dinophyceae): mycosporine-like amino  
691 acids protect against inhibition of photosynthesis. *J Phycol*, 34, 928-938, 1998.
- 692 33. Neale, P. J., and Thomas, B. C.: Inhibition by ultraviolet and photosynthetically  
693 available radiation lowers model estimates of depth-integrated picophytoplankton  
694 photosynthesis: global predictions for *Prochlorococcus* and *Synechococcus*, *Glob*  
695 *Change Biol*, 13356, 10.1111/gcb.13356, 2016.
- 696 34. Olson, E. M., McGillicuddy, D. J., Dyrman, S. T., Waterbury, J. B., Davis, C. S.,  
697 and Solow, A. R.: The depth-distribution of nitrogen fixation by *Trichodesmium*

- 698 spp. colonies in the tropical–subtropical North Atlantic, Deep Sea Research Part I:  
699 Oceanographic Research Papers, 104, 72-91, 10.1016/j.dsr.2015.06.012, 2015.
- 700 35. Prufert-Bebout, L., Paerl, H. W., and Lassen, C.: Growth, nitrogen fixation, and  
701 spectral attenuation in cultivated *Trichodesmium* species, Appl Environ Microb, 59,  
702 1367-1375, 1993.
- 703 36. Quesada, A., Vincent, W. F., and Lean, D. R. S.: Community and pigment structure  
704 of Arctic cyanobacterial assemblages: the occurrence and distribution of UV-  
705 absorbing compounds, FEMS Microbiol. Ecol., 28, 315-323, 10.1111/j.1574-  
706 6941.1999.tb00586.x, 1999.
- 707 37. Rastogi, R. P., Sinha, R. P., Moh, S. H., Lee, T. K., Kottuparambil, S., Kim, Y. J.,  
708 Rhee, J. S., Choi, E. M., Brown, M. T., Hader, D. P., and Han, T.: Ultraviolet  
709 radiation and cyanobacteria, J. Photochem. Photobiol. B: Biol., 141, 154-169,  
710 10.1016/j.jphotobiol.2014.09.020, 2014.
- 711 38. Rath, J., and Adhikary, S. P.: Response of the estuarine cyanobacterium *Lyngbya*  
712 *aestuarii* to UV-B radiation, J Appl Phycol, 19, 529-536, 2007.
- 713 39. Ritchie, R. J.: Consistent sets of spectrophotometric chlorophyll equations for  
714 acetone, methanol and ethanol solvents, Photosyn. Res., 89, 27-41,  
715 10.1007/s11120-006-9065-9, 2006.
- 716 40. Shi, D., Kranz, S. A., Kim, J. M., and Morel, F. M. M.: Ocean acidification slows  
717 nitrogen fixation and growth in the dominant diazotroph *Trichodesmium* under  
718 low-iron conditions, Proceedings of the National Academy of Sciences, 109,  
719 E3094-E3100, 2012.
- 720 41. Shick, J. M., and Dunlap, W. C.: Mycosporine-like amino acids and related  
721 Gadusols: biosynthesis, accumulation, and UV-protective functions in aquatic  
722 organisms, Annu Rev Physiol, 64, 223-262,  
723 10.1146/annurev.physiol.64.081501.155802, 2002.
- 724 42. Singh, Shailendra P., Sunita Kumari, Rajesh P. Rastogi, Kanchan L. Singh, and  
725 Rajeshwar P. Sinha.: Mycosporine-like amino acids (MAAs): chemical structure,

- 726 biosynthesis and significance as UV-absorbing/screening compounds, *Indian J*  
727 *Exp Biol*, 46, 7-17, 2008.
- 728 43. Singh, S. P., Rastogi, R. P., Hader, D. P., and Sinha, R. P.: Temporal dynamics of  
729 ROS biogenesis under simulated solar radiation in the cyanobacterium *Anabaena*  
730 *variabilis* PCC 7937, *Protoplasma*, 251, 1223-1230, 10.1007/s00709-014-0630-3,  
731 2014.
- 732 44. Sinha, R. P., Singh, N., Kumar, A., Kumar, H. D., Häder, M., and Häder, D. P.:  
733 Effects of UV irradiation on certain physiological and biochemical processes in  
734 cyanobacteria, *J. Photochem. Photobiol. B: Biol.*, 32, 107-113,  
735 [http://dx.doi.org/10.1016/1011-1344\(95\)07205-5](http://dx.doi.org/10.1016/1011-1344(95)07205-5), 1996.
- 736 45. Sinha, R. P., Singh, N., Kumar, A., Kumar, H. D., and Häder, D.-P.: Impacts of  
737 ultraviolet-B irradiation on nitrogen-fixing cyanobacteria of rice paddy fields, *J*  
738 *Plant Physiol*, 150, 188-193, [http://dx.doi.org/10.1016/S0176-1617\(97\)80201-5](http://dx.doi.org/10.1016/S0176-1617(97)80201-5),  
739 1997.
- 740 46. Sinha, R. P., Klisch, M., Walter Helbling, E., and Häder, D.-P.: Induction of  
741 mycosporine-like amino acids (MAAs) in cyanobacteria by solar ultraviolet-B  
742 radiation, *J. Photochem. Photobiol. B: Biol.*, 60, 129-135,  
743 [http://dx.doi.org/10.1016/S1011-1344\(01\)00137-3](http://dx.doi.org/10.1016/S1011-1344(01)00137-3), 2001.
- 744 47. Sinha, R. P., Ambasht, N. K., Sinha, J. P., Klisch, M., and Häder, D.-P.: UV-B-  
745 induced synthesis of mycosporine-like amino acids in three strains of *Nodularia*  
746 (cyanobacteria), *J. Photochem. Photobiol. B: Biol.*, 71, 51-58,  
747 <http://dx.doi.org/10.1016/j.jphotobiol.2003.07.003>, 2003.
- 748 48. Sinha, R. P., and Häder, D.-P.: UV-protectants in cyanobacteria, *Plant Sci.*, 174,  
749 278-289, 10.1016/j.plantsci.2007.12.004, 2008.
- 750 49. Sobrino, C., and Neale, P. J.: Short-term and long-term effects of temperature on  
751 photosynthesis in the diatom *Thalassiosira Pseudonana* under UVR exposures, *J*  
752 *Phycol*, 43, 426-436, 10.1111/j.1529-8817.2007.00344.x, 2007.
- 753 50. Sohm, J. A., Webb, E. A., and Capone, D. G.: Emerging patterns of marine nitrogen

- 754 fixation, *Nat Rev Microbiol*, 9, 499-508, 10.1038/nrmicro2594, 2011.
- 755 51. Spungin, D., Berman-Frank, I., and Levitan, O.: *Trichodesmium's* strategies to  
756 alleviate P-limitation in the future acidified oceans, *Environ. Microbiol.*, 16,  
757 1935-1947, 10.1111/1462-2920.12424, 2014.
- 758 52. Subramaniam, A., Carpenter, E. J., Karentz, D., and Falkowski, P. G.: Bio-optical  
759 properties of the marine diazotrophic cyanobacteria *Trichodesmium* spp. I.  
760 Absorption and photosynthetic action spectra, *Limnol Oceanogr*, 44, 608-617,  
761 1999.
- 762 53. Vernet, M., and Whitehead, K.: Release of ultraviolet-absorbing compounds by the  
763 red-tide dinoflagellate *Lingulodinium polyedra*, *Mar. Biol.*, 127, 35-44,  
764 10.1007/bf00993641, 1996.
- 765 54. Villafañe, V. E., Barbieri, E. S., and Helbling, E. W.: Annual patterns of ultraviolet  
766 radiation effects on temperate marine phytoplankton off Patagonia, Argentina, *J*  
767 *Plankton Res*, 26, 167-174, 10.1093/plankt/fbh011, 2004.
- 768 55. Westberry, T. K., and Siegel, D. A.: Spatial and temporal distribution of  
769 *Trichodesmium* blooms in the world's oceans, *GBioC*, 20, GB4016,  
770 10.1029/2005gb002673, 2006.
- 771 56. Wu, H., Gao, K., Villafane, V. E., Watanabe, T., and Helbling, E. W.: Effects of  
772 solar UV radiation on morphology and photosynthesis of filamentous  
773 cyanobacterium *Arthrospira platensis*, *Appl Environ Microb*, 71, 5004-5013,  
774 10.1128/AEM.71.9.5004-5013.2005, 2005.
- 775 57. Wu, H., Abasova, L., Cheregi, O., Deák, Z., Gao, K., and Vass, I.: D1 protein  
776 turnover is involved in protection of Photosystem II against UV-B induced damage  
777 in the cyanobacterium *Arthrospira (Spirulina) platensis*, *J. Photochem. Photobiol.*  
778 *B: Biol.*, 104, 320-325, <http://dx.doi.org/10.1016/j.jphotobiol.2011.01.004>, 2011.
- 779 58. Wu, Y., Li, Z., Du, W., and Gao, K.: Physiological response of marine centric  
780 diatoms to ultraviolet radiation, with special reference to cell size, *J. Photochem.*  
781 *Photobiol. B: Biol.*, 153, 1-6, <http://dx.doi.org/10.1016/j.jphotobiol.2015.08.035>,



782 2015.

783